ACS Catalysis

pubs.acs.org/acscatalysis

Research Article

Compressive Strain Reduces the Hydrogen Evolution and Oxidation Reaction Activity of Platinum in Alkaline Solution

Li Jiao, Ershuai Liu, Sooyeon Hwang, Sanjeev Mukerjee, and Qingying Jia*

Cite This: *ACS Catal.* 2021, 11, 8165–8173

Read Online

ACCESS | Metrics & More | Article Recommendations | Supporting Information

ABSTRACT: It is unclear why the hydrogen evolution and oxidation reactions (HER/HOR) of platinum (Pt) are much slower in base than in acid. Neither is it clear why the sluggish HER/HOR of Pt in a base can be improved by mixing Pt with some transition metals. Herein, we constructed dealloyed carbon-supported Pt−Cu nanoclusters (D-$PtCu_3$/C) with a core−shell Cu@Pt structure wherein the Pt−Cu alloying core is surrounded by Pt shells as a model HER/HOR catalyst to interpret these puzzles. Combined microscopy and *in situ* X-ray absorption spectroscopy verified the Cu@Pt structure in association with the compressive strain in D-$PtCu_3$/C during the HER/HOR. The superior oxygen reduction reaction activity of the D-$PtCu_3$/C to that of Pt/C in both acid and alkaline solution confirmed that the compressive strain weakens the Pt−O binding energy (E_{Pt-O}) of the D-$PtCu_3$/C. The D-$PtCu_3$/C with compressed Pt shells exhibited inferior HER/HOR activity and a positive shift of the sharp hydrogen adsorption/desorption peaks toward higher potential in comparison with Pt/C in alkaline solution. These results verified that the compressive strain reduces the HER/HOR activity of Pt by weakening E_{Pt-O}. This conclusion indicates that the HER/HOR kinetics of Pt in a base is mainly limited by the overly weak E_{Pt-O} rather than overly strong Pt−H binding energy.

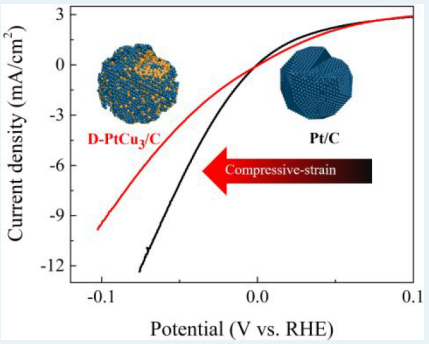

KEYWORDS: *HER/HOR, platinum catalyst, core−shell structure, XAS, interface*

1. INTRODUCTION

The kinetics of the hydrogen evolution and oxidation reactions (HER/HOR) of platinum (Pt) in the alkaline solution with a pH value of 13 is 2 orders of magnitude lower than that in the acid solution with a pH value of 0.[1] Consequently, high loading of Pt is required in alkaline electrolyzers and fuel cells to sufficiently boost the HER and HOR, respectively, which contributes substantially to the high costs of these devices. Efforts to reduce Pt loading in these devices by improving the HER/HOR activity of Pt in a base have been hindered by poor understanding of the sluggish HER/HOR kinetics of Pt in a base. Moreover, the lack of clear understanding of these most fundamental electrochemical reactions is indicative of a critical knowledge gap in electrochemistry. Elucidating the reason(s) behind the sluggish HER/HOR kinetics of Pt in a base is thus both practically and fundamentally important.

One major strategy to understand the sluggish HER/HOR kinetics of Pt in alkaline solution is to improve the HER/HOR activity of Pt by mixing it with a second transition metal such as ruthenium (Ru) and nickel (Ni), followed by elucidating the underlying mechanism(s) for the improvement. However, this strategy has not led to conclusive explanations of the sluggish HER/HOR kinetics of Pt in a base, mainly because the promoting roles of the mixed metal are elusive. Many groups showed that depositing small amounts of Ru or Ni on Pt surfaces can significantly boost their HER and/or HOR activity in alkaline solution.[2−9] However, the proposed promoting roles of the surface Ru or Ni differ dramatically. They include but are not limited to facilitating water dissociation,[6,8] promoting hydroxide adsorption/desorption,[2−4,8] shifting the potential of zero free charge (pzfc),[9] or reorientating interfacial water molecules.[2] In this regard, a comprehensive and in-depth discussion can be found in a recent article by Tang et al.[10] These proposed roles are all theoretically possible since the surface Ru or Ni is exposed within the double-layer interface wherein it may interact with the Pt surface, interfacial water, HER/HOR intermediates, alkali cations, and hydroxides in the electrolyte. These interactions are potential dependent since the electric interfacial field is potential dependent, plus the surface Ru and Ni are redox active within the HER/HOR potentials.[2] *In situ* characterization of the complex electrode−electrolyte interface across multiple spatial and temporal scales is therefore required to conclusively identify and deconvolute the promoting roles of the surface Ru or Ni on the HER/HOR

Received: April 15, 2021
Revised: June 6, 2021
Published: June 18, 2021

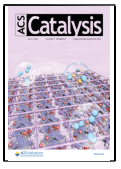

https://doi.org/10.1021/acscatal.1c01723
ACS Catal. 2021, 11, 8165−8173

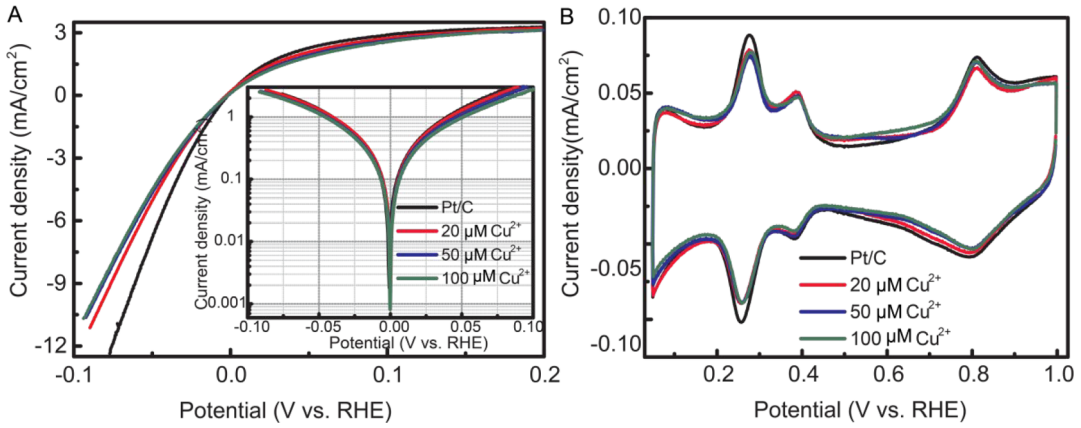

Figure 1. (A) *iR*-corrected HOR/HER polarization curves (negative-going scans) of the Pt/C (10 $\mu g/cm^2$) electrode with/without surface deposition of $Cu(ClO_4)_2$ in an H_2-saturated 0.1 M KOH electrolyte at room temperature. Scan rate: 10 $mV{\cdot}s^{-1}$. Rotation rate: 2500 rpm. The Pt/C electrode was orderly immersed in $Cu(ClO_4)_2$ solution at a variety of concentrations. The Tafel plots (Figure 1A, inset) were derived from the *iR*-corrected polarization curves and corrected for hydrogen mass transport in the HOR branch using the Koutecky–Levich equation and the H_{upd} charges integrated from 0.05 to 0.45 V in the cyclic voltammetry (CV) in (B). (B) CV of the Pt/C electrode collected in Ar-saturated 0.1 M KOH with/without surface deposition of $Cu(ClO_4)_2$ with a scan rate of 10 mV/s.

kinetics of Pt in alkaline solution. Such advanced characterization is, however, beyond current experimental capabilities.

On the other hand, it was reported that the Pt–Ru[11−13] and Pt–Ni[14] nanoparticles with the Ru or Ni exclusively in the core surrounded by pure Pt shells (so-called core–shell structure denoted as M@Pt, M = Ni, Ru, or other transition metals) exhibited HER/HOR activity superior to that of Pt in alkaline solution. The activity improvement was attributed to the Ru or Ni induced weakening of the Pt–H binding energy (E_{Pt-H}) via the compressive-strain and/or ligand effects *as per* the hydrogen binding energy (HBE) theory.[11,14] According to this theory, the slower HER/HOR kinetics of Pt in base than in acid is because the E_{Pt-H} increases with increasing pH and becomes too strong for the Volmer step in high pH media: $Pt-H_{ad} + OH^- \leftrightarrow Pt + H_2O + e^-$.[1,15−17] The claim that the Ru or Ni buried underneath the surface improves the HER/HOR activity of Pt exclusively supports the HBE theory, since all other proposed promoting roles of Ru or Ni mentioned above require it to be located on the electrode surface exposed to the double-layer interface. The core–shell structure of M@Pt greatly eases the characterization in comparison with the Pt–M structures with surface M. This is because the M buried in the core is electrochemically inactive and not exposed in the interface, so its only means to modify the HER/HOR activity of Pt is via modification of the electronic properties of the Pt surface. Therefore, the M@Pt structure represents a relatively well-defined platform to study the HER/HOR kinetics of the Pt in a base. However, the Ru@Pt and Ni@Pt used as model HER/HOR catalysts have a critical issue, that is, even trace amounts of Ru or Ni on Pt surfaces can dramatically boost the HER and/or HOR activity of Pt in an alkaline solution.[2−5,7,8] *Ex situ* characterization cannot rule out the presence of trace amounts of Ru or Ni on the surface of Ru@Pt or Ni@Pt. Even if it did, Ru and Ni have a strong tendency to migrate onto the surface under *in situ* electrochemical conditions with applied potentials due to their relatively high oxophilicity.[18,19] It therefore remains debatable whether the improved HER/HOR activity of Ru@Pt and Ni@Pt arises from the Ru or Ni buried in the core or exposed on the surface or a combination thereof. This ambiguity makes the arguments based on the Ru@Pt and Ni@Pt structures with presumably clean Pt surfaces free of Ru or Ni inconclusive.

In light of the merits and limitations of Ru@Pt and Ni@Pt as model HER/HOR catalysts, we constructed Cu@Pt nanoclusters as a model catalyst to study the compressive-strain effect on the HER/HOR kinetics of Pt in alkaline solution in this work. We chose Cu because it compresses Pt shells like Ru and Ni, but unlike Ru and Ni the Cu on the Pt surface does not significantly alter the HER/HOR kinetics of Pt in alkaline solution. We found that the Cu-induced compressive strain in Cu@Pt reduces the HER/HOR activity of Pt in alkaline solution and shifts the sharp underpotential-deposited hydrogen (H_{upd}) peaks of Pt anodically toward higher potential. These experimental results show that the compressive strain reduces the HER/HOR activity of Pt in alkaline by weakening the Pt–O binding energy (E_{Pt-O}), rather than improving the HER/HOR activity of Pt in alkaline by weakening E_{Pt-H} as commonly believed. We accordingly propose that the sluggish HER/HOR kinetics of Pt in alkaline solution is owing primarily to the overly weak E_{Pt-O}. The implications of this argument for the HER/HOR kinetics of Pt in a base are discussed.

2. RESULTS

We first evaluated the effects of the surface Cu on the HER/HOR kinetics of Pt in alkaline by immersing a commercial Pt/C (Tanaka Kikinzoku Kogyo, 47.2%) electrode in $Cu(ClO_4)_2$ solution with a variety of concentrations following our previous protocol for surface metal deposition.[3] The Cu coverage on the Pt/C increases with increasing $Cu(ClO_4)_2$ concentration.[2,3] The HOR/HER polarization curves (*iR*-corrected) of the bare and Cu-deposited Pt/C electrode (Figure 1A) are obtained by rotating disk electrode (RDE) in H_2-saturated 0.1 M KOH electrolyte (99.99%). The corresponding cyclic voltammetry (CV) results are displayed in Figure 1B. As seen, both the HOR/HER rates of Pt/C and the H_{upd} charge decrease with increasing $Cu(ClO_4)_2$ concentration. These trends indicate that the surface Cu reduces the HER/HOR rates of Pt/C by blocking Pt sites. The HER/HOR kinetic currents, which are obtained by normalizing the HER/HOR measured currents by the electrochemical surface area (ECSA) derived from

https://doi.org/10.1021/acscatal.1c01723
ACS Catal. 2021, 11, 8165−8173

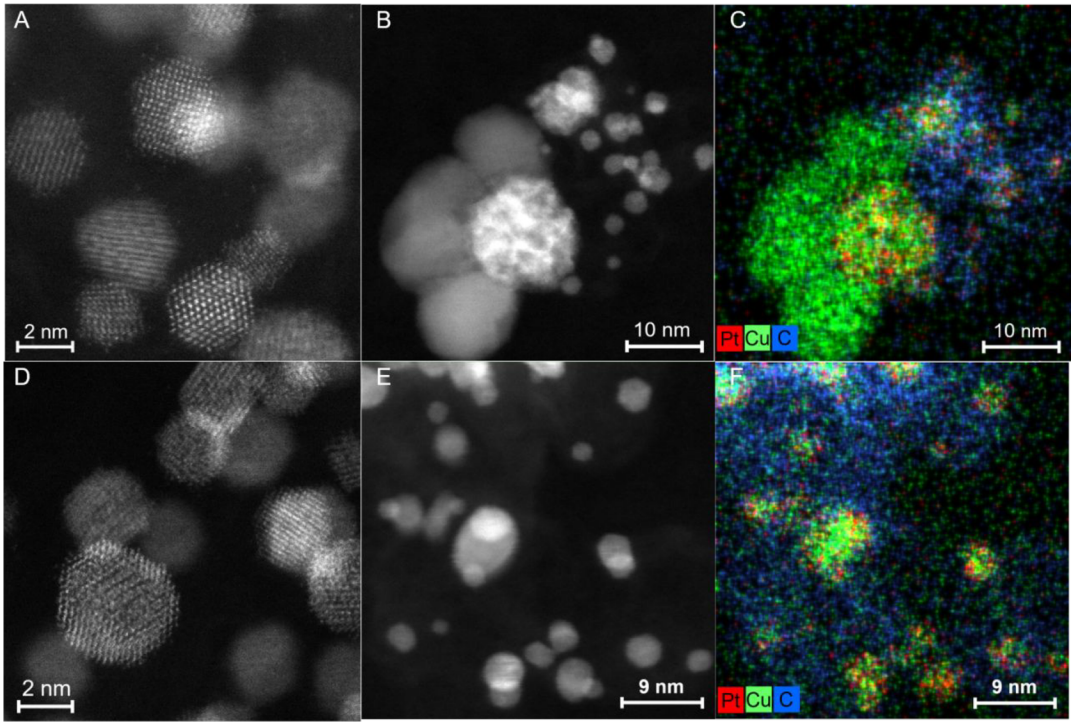

Figure 2. HAADF-STEM images and STEM-EDS elemental maps of as-synthesized $PtCu_3/C$ (A, B, C) and D-$PtCu_3/C$ catalysts (D, E, F). Red, green, and blue colors represent Pt, Cu, and C, respectively.

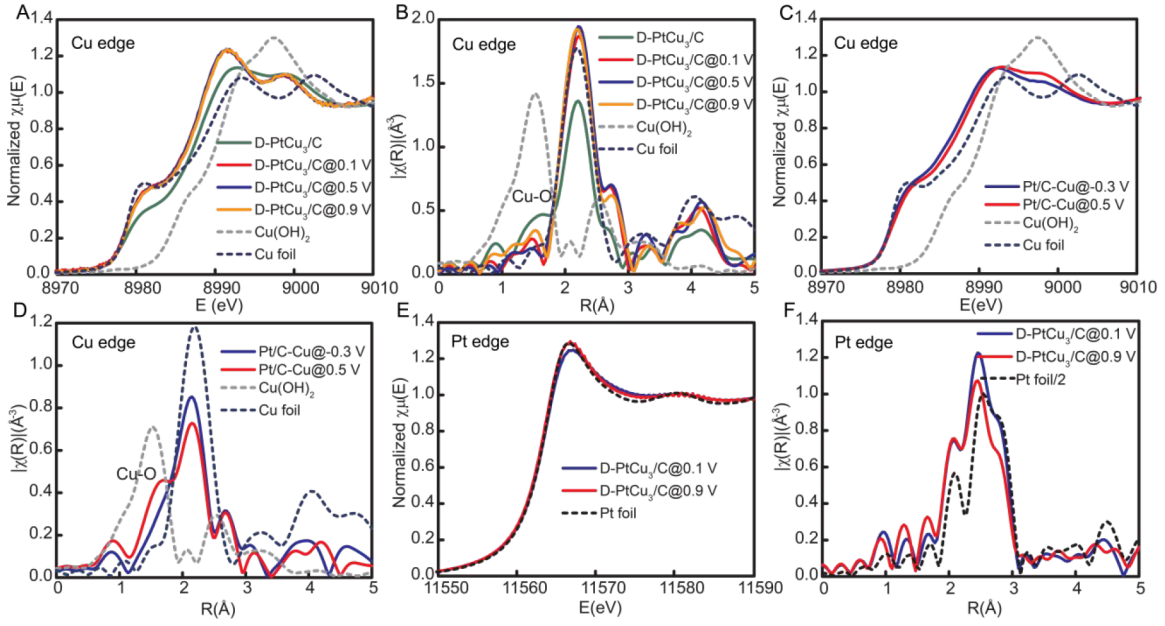

Figure 3. Cu K-edge (A) XANES and (B) FT-EXAFS spectra of the D-$PtCu_3/C$ collected in an H_2-saturated 0.1 M KOH electrolyte at various potentials, as well as of the as-synthesized $PtCu_3/C$, $Cu(OH)_2$, and Cu foil standards for comparison. The Cu K-edge (C) XANES and (D) FT-EXAFS spectra of the Cu deposited onto Pt/C collected in an H_2-saturated 0.1 M KOH electrolyte at various potentials, as well as of the $Cu(OH)_2$ and Cu foil standards for comparison. The Pt L_3-edge (E) XANES and (F) FT-EXAFS spectra of the D-$PtCu_3/C$ collected in an H_2-saturated 0.1 M KOH electrolyte at various potentials, as well as of the Pt foil standards for comparison.

integrating the H_{upd} charge from 0.05 to 0.45 V (all potentials reported here are referenced to the reversible hydrogen electrode), decrease slightly with increasing $Cu(ClO_4)_2$ concentration (Figure 1A, inset). This is likely because the surface Cu selectively blocks the Pt(110) facet that has intrinsic HER/HOR activity superior to those of the Pt(111) and Pt (100) facets,[20] as reflected by the selective decrease of the intensity of the hydrogen adsorption/desorption peaks of the Pt(110) facet around 0.28 V (Figure 1B). These results confirm that the surface Cu has negligible effects on the HOR/HER kinetics of Pt. The same result was previously obtained by depositing Cu onto a Pt polycrystalline electrode, whereas depositing Mn, Fe, Co, Ni, and Ru clearly modified the HER and/or HOR kinetics of Pt.[2] The negligible effects of the

https://doi.org/10.1021/acscatal.1c01723
ACS Catal. 2021, 11, 8165−8173

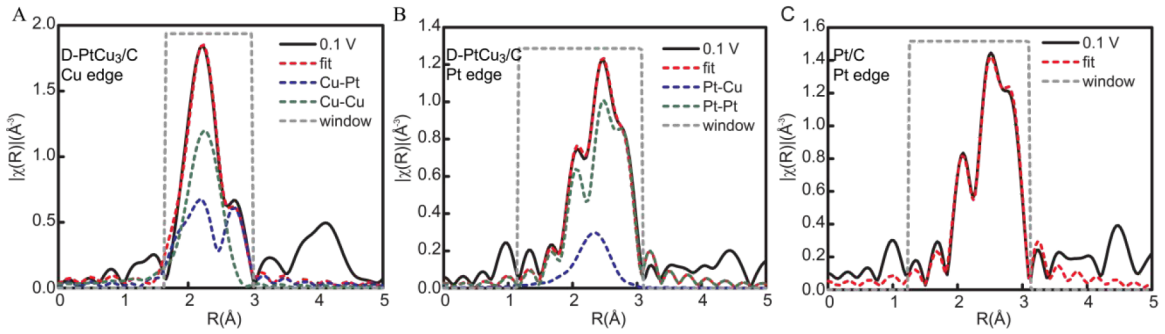

Figure 4. FT-EXAFS spectra and the corresponding fits of the D-$PtCu_3$/C collected in an H_2-saturated 0.1 M KOH electrolyte at 0.1 V at the (A) Cu K-edge and (B) Pt L_3-edge. (C) The FT-EXAFS spectra and the corresponding fits of the Pt/C collected in an H_2-saturated 0.1 M KOH electrolyte at 0.1 V at the Pt L_3-edge.

surface Cu on the HOR/HER kinetics of Pt in alkaline solution constitutes the premise of the choice of Cu@Pt as a model HER/HOR catalyst in this work.

We constructed the Cu@Pt nanoclusters by chemically dealloying the carbon supported $PtCu_3$ nanoparticles (D-$PtCu_3$/C). The synthesis of $PtCu_3$/C and its basic properties such as mean particle size and composition can be found in the previous report.[21] The detailed chemical dealloying process is given in the Experimental Methods section. High-angle annular dark-field scanning transmission electron microscopy (HAADF-STEM) imaging shows that the dealloying process did not change the shape and particle size of $PtCu_3$/C significantly (Figure 2A vs Figure 2D). In the as-synthesized $PtCu_3$/C, particles with predominately Cu were observed, which is expected from the high content of Cu in the $PtCu_3$/C precursor (Figure 2B and Figure 2C). These particles were not observed after dealloying, whereas particles with Cu concentrated in the cores emerged (Figure 2E and Figure 2F). These Cu-enriched cores were covered by Pt shells with the thickness in the range of 0.7−1.2 nm as shown by the linear scanning imaging (Figure S1). These results indicate the selective removal of Cu from the outer surfaces of $PtCu_3$/C by acidic dealloying, consistent with previous observations on the dealloying of $PtCu_3$/C.[21]

Next, we show that the *Cu@Pt* structure is preserved under *in situ* HER/HOR conditions by conducting *in situ* X-ray absorption spectroscopy (XAS) on the D-$PtCu_3$/C catalyst. The as-synthesized $PtCu_3$/C catalyst and the commercial Pt/C with and without surface deposition of Cu (Pt/C−Cu) were also measured for comparison. Extended X-ray absorption fine structure (EXAFS) and X-ray absorption near-edge structure (XANES) spectra were collected at both the Cu K-edge and Pt L_3-edge to determine the structure of the D-$PtCu_3$/C from both the Cu and the Pt perspectives. The *ex situ* Cu XANES spectrum of D-$PtCu_3$/C is located between that of the Cu foil and that of $Cu(OH)_2$ (Figure 3A). Meanwhile, the Fourier transform of the EXAFS spectrum exhibits a prominent peak around 2.2 Å (without phase correction) overlapping the first-shell Cu−Cu scattering peak of the Cu foil, as well as a small peak around 1.5 Å overlapping the Cu−O scattering peak of the $Cu(OH)_2$ (Figure 3B). These results confirm that the Cu in the as-synthesized $PtCu_3$/C is in the mixed forms of metallic Cu and $Cu(OH)_2$. The copresence of oxidative and metallic phases is typical for PtM nanoparticles in which the M exposed on the surface and buried in the core is normally in the oxidative and reduced metallic phase, respectively.[21,22]

After the chemically dealloying process of the $PtCu_3$/C powders, the produced D-$PtCu_3$/C was subjected to acid conditioning followed by *in situ* XAS measurements as a function of the applied potentials in an H_2-saturated 0.1 M KOH electrolyte. The *in situ* XANES spectra of the D-$PtCu_3$/C shift negatively toward lower energy compared with the *ex situ* XANES spectrum of the D-$PtCu_3$/C, overlapping that of the Cu foil (Figure 3A). Concomitantly the Cu−O scattering peak around 1.5 Å vanishes in the *in situ* FT-EXAFS spectra of the D-$PtCu_3$/C, and the peak around 2.2 Å grows (Figure 3B). These results show the absence of the $Cu(OH)_2$ in the D-$PtCu_3$/C *in situ* during the HER/HOR, and the Cu in the D-$PtCu_3$/C is mainly in the reduced metallic phase. In addition, the *in situ* XANES and FT-EXAFS spectra of the D-$PtCu_3$/C remain unchanged within the potential range of 0.1−0.9 V (Figure 3A,B). In contrast, the *in situ* XANES spectrum of the surface deposited Cu on Pt/C undergoes a small but definitive shift toward higher energy as the potential increases from −0.3 to 0.5 V (Figure 3C), which indicates oxidation of the surface deposited Cu. The Cu oxidation is also reflected by the growth of the peak of the XANES spectrum around 8998 V (Figure 3C). This peak is present in the XANES spectrum of $Cu(OH)_2$ and indicative of charge transfer from Cu to O. Furthermore, the Cu−O scattering peak around 1.5 Å emerges in the *in situ* FT-EXAFS spectrum as the potential increases from −0.3 to 0.5 V (Figure 3D). These results confirm that the Cu on the Pt surface is electroactive and undergoes a redox transition between Cu^0 and $Cu(OH)_2$ within the HER/HOR potential region. Therefore, the unchanged *in situ* XAS spectra of the Cu in the D-$PtCu_3$/C and the absence of the Cu−O scattering peak within the potential range of 0.1−0.9 V confirm that the Cu in the D-$PtCu_3$/C is buried in the core and electrochemically inactive.

On the other hand, the white line intensity of the *in situ* XANES spectra at the Pt L_3-edge of the D-$PtCu_3$/C increases as the potential increases to 0.9 V (Figure 3E), and the intensity of the FT-EXAFS spectra decreases (Figure 3F). The same trends were also observed on Pt/C.[23] These phenomena have been commonly observed during the *in situ* XAS measurements on Pt alloys and are well-known as an indication of the adsorption of O(H) species onto Pt surfaces at elevated potentials.[23,24] Therefore, these *in situ* XAS results verify the core−shell Cu@Pt structure of the D-$PtCu_3$/C wherein the Cu is in the core surrounded by pure Pt shells during the HER/HOR.

The core−shell Cu@Pt structure of D-$PtCu_3$/C is further confirmed by fitting the FT-EXAFS spectra of the D-$PtCu_3$/C

https://doi.org/10.1021/acscatal.1c01723
ACS Catal. 2021, 11, 8165−8173

collected at 0.1 V at the Pt and Cu edges simultaneously. The FT-EXAFS spectra of both the Cu (Figure 4A) and Pt (Figure 4B) edges can be well fitted by using a Pt−Cu cluster model, which shows that both the Pt and the Cu in the D-PtCu$_3$/C are predominately in the reduced alloying phase. The higher total coordination number (N) of Cu ($N_{Cu} = N_{Cu-Cu} + N_{Cu-Pt}$) compared with that of Pt ($N_{Pt} = N_{Pt-Cu} + N_{Pt-Pt}$) (Table 1) supports the core−shell Cu@Pt structure since geometrically the surface sites have lower coordination numbers than the sites in the core. More importantly, the first-shell bulk-average Pt−Pt bond length (R_{Pt-Pt}) of the D-PtCu$_3$/C (2.725 ± 0.004 Å) is ∼1.1% shorter than that of Pt/C (2.756 ± 0.002 Å). These results verify the Cu-induced compressive strain in the D-PtCu$_3$/C with a core−shell Cu@Pt structure, thereby further justifying the usage of the D-PtCu$_3$/C as a model HER/HOR catalyst from the structure perspective.

Table 1. Summaries of EXAFS Fitting Results of D-PtCu$_3$/C at 0.1 V in H$_2$-Saturated 0.1 M KOH Electrolyte[a]

catalyst	bond type	R (Å)	N	$\sigma^2 \times 10^{-3}$ (Å^2)
D-PtCu$_3$/C	Pt−Pt	2.725 ± 0.004	7.5 ± 0.7	5.9 ± 0.5
	Pt−Cu	2.66 ± 0.01	1.6 ± 0.7	9 ± 3
	Cu−Pt	2.66 ± 0.01	5.3 ± 1.7	9 ± 3
	Cu−Cu	2.61 ± 0.02	5.6 ± 2.3	11 ± 3
Pt/C	Pt−Pt	2.756 ± 0.002	9.0 ± 0.6	5.0 ± 0.3

[a] S_0^2 was fixed at 0.87 and 1.0 for Pt and Cu, respectively, as obtained by fitting the corresponding reference foils. Fits were done in R-space, $k^{1,2,3}$ weighting. 1.15 < R < 3.10 Å and Δk = 2.68−13.50 Å^{-1} were used for fitting the Pt L$_3$-edge spectra, and 1.63 < R < 3.00 Å and Δk = 2.70−11.00 Å^{-1} were used for fitting the Cu K-edge spectra. The fitting results of the E_0 at the Pt L$_3$- and Cu K-edges are 7.5 ± 0.5 eV and −2.4 ± 1.4 eV, respectively. The fitting result of the E_0 at the Pt L$_3$-edge FT-EXAFS spectrum of Pt/C is 6.8 ± 0.5 eV.

Next, we show that the Cu-induced compressive strain has profound influences on the catalytic activities of the D-PtCu$_3$/C by assessing the oxygen reduction reaction (ORR) activities of the D-PtCu$_3$/C in O$_2$-saturated 0.1 M HClO$_4$ followed by in 0.1 M KOH. In both electrolytes, the D-PtCu$_3$/C exhibits an intrinsic ORR activity superior to that of Pt/C (Figure 5A,B). This result is fully expected since acidic dealloying of PtCu$_3$/C powders leading to a core−shell Cu@Pt structure and improved ORR activity was originally demonstrated by Strasser et al.[25] Numerous reports later expanded the Cu@Pt to M@Pt (M = Co, Ni, Cu, or Ru) and concluded that the improved ORR activity of M@Pt is caused by the M-induced compressive strain that weakens the E_{Pt-O} by downshifting the Pt d-band center relative to the Fermi level.[24,26] The compressive-strain induced downshift of the Pt d-band center weakens not only the E_{Pt-O} but also the E_{Pt-H} as per the d-band theory.[27−29] The improved HER and/or HOR activity of

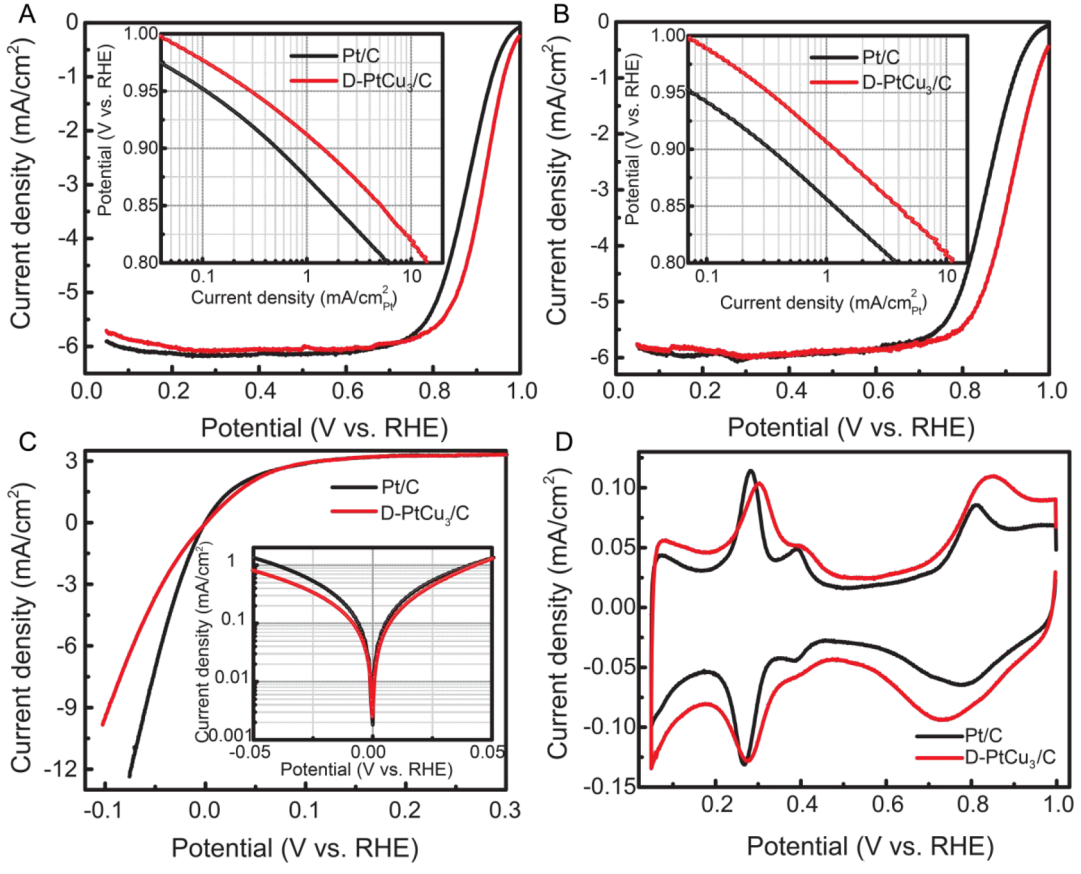

Figure 5. ORR polarization curves of the D-PtCu$_3$/C and Pt/C obtained in (A) O$_2$-saturated 0.1 M HClO$_4$ and (B) O$_2$-saturated 0.1 M KOH with a rotating rate of 1600 rpm and scan rate of 10 mV/s. (C) The HER/HOR polarization curves of the D-PtCu$_3$/C and Pt/C obtained in H$_2$-saturated 0.1 M KOH with a rotating rate of 2500 rpm and a scan rate of 10 mV/s. The corresponding Tafel plots with the kinetic current normalized by the ECSA derived from the H$_{upd}$ charge are displayed in the insets of (A)−(C). (D) CV of the D-PtCu$_3$/C and Pt/C electrodes in an Ar-saturated 0.1 M KOH electrolyte with a scan rate of 10 mV/s.

https://doi.org/10.1021/acscatal.1c01723
ACS Catal. 2021, 11, 8165−8173

Ru@Pt and Ni@Pt in alkaline solution has been commonly ascribed to the compressive strain induced weakening of the E_{Pt-H}.[11−14,30] This argument supports the HBE theory by acknowledging the overly strong E_{Pt-H} as the major cause of the sluggish HER/HOR kinetics of Pt in a base.[1,15−17] Therefore, the D-PtCu$_3$/C with a compressed Cu@Pt structure is expected to exhibit improved HER/HOR activity as per the HBE theory.

However, the D-PtCu$_3$/C electrode that exhibits superior ORR activity to Pt/C shows inferior intrinsic HER/HOR activity to Pt/C in subsequent measurements in H$_2$-saturated 0.1 M KOH (Figure 5C). The D-PtCu$_3$/C has minimal amounts of surface Cu (if at all) during the HER/HOR (Figure 3), which is further supported by essentially the same HOR limiting currents between the D-PtCu$_3$/C and the Pt/C (Figure 5C), and the poisoning effect of the surface Cu can be ruled out. In addition, the surface Cu has minimal impacts on the HER/HOR kinetics of Pt in 0.1 M KOH (Figure 1). Therefore, the appreciably lower intrinsic HER/HOR activity of the D-PtCu$_3$/C compared with that of Pt/C can be ascribed to the Cu-induced compressive strain. These results show that the compressive strain reduces the HER/HOR intrinsic activity of Pt in alkaline solution, in contrast to previous reports. More importantly, this conclusion challenges the widely accepted HBE theory, which we elaborate next.

3. DISCUSSION

In this section we try to provide a reason why the compressive strain decreases the HER/HOR intrinsic activity of the Pt in alkaline solution and then draw a conclusion on the cause of the sluggish HER/HOR activity of Pt in a base based on the reasoning. The HER/HOR of Pt in a base is limited by the Volmer step:[1,8,31,32]

$$Pt{-}H_{ad} + OH^- \leftrightarrow Pt + H_2O + e^- \quad (1)$$

Weakening E_{Pt-H} is believed to promote the Volmer step according to the density functional theory calculations (DFT) that the E_{Pt-H} is ∼0.2 eV, which is overly strong.[8] On the other hand, weakening E_{Pt-O} may slow down the Volmer step of Pt in a base if it is limited by the overly weak E_{Pt-O} as recently proposed by our group[2] and Koper's group.[8] Koper's group showed by DFT calculations that the E_{Pt-OH} values of Pt(111) and Pt(553) are ∼0.9 eV and ∼0.3 eV, which are overly weak, respectively.[8] Since the compressive strain weakens both the E_{Pt-H} and the E_{Pt-O} by downshifting the Pt d-band relative to the Fermi level, the observation that the Cu-induced compressive strain decreases the HER/HOR activity of Pt in alkaline solution indicates that the promoting effect of weakening E_{Pt-H} (if at all) is overwhelmed by the detrimental effect of weakening E_{Pt-O}. This inference is further supported by the observation that the Pt(110) H_{upd} peaks of the D-PtCu$_3$/C are located ∼20 mV more positive relative to those of Pt/C (Figure 5D). The shift of the Pt(110) H_{upd} peak position is caused by the Cu in the core since the surface deposited Cu does not shift the H_{upd} peaks but just reduces their intensity (Figure 1B). Although the explicit causes of these H_{upd} peaks are currently under debate, they involve the adsorption/desorption of H_{ad} and are therefore closely related to the Volmer step. Yan's group previously showed that the H_{upd} peaks of the Pt polycrystalline electrode shift anodically with increasing pH, and their position (E_{peak}) is linearly related to the HER/HOR activity of the Pt polycrystalline electrode within a pH range of 0−13.[15] They further proposed that the E_{peak} is linearly related to the E_{Pt-H} and accordingly proposed the HBE theory that the HER/HOR activity of the Pt is solely governed by the E_{Pt-H} and decreases with increasing E_{Pt-H} as the pH increases. According to this argument, weakening E_{Pt-H} shall improve the HER/HOR activity of the Pt and meanwhile negatively shift the E_{peak}, both opposite to the experimental observations shown here. Yan's group later rectified the HBE theory stating that the E_{peak} is linearly related to the difference in E_{Pt-H} and E_{Pt-H2O} (so-called apparent hydrogen binding energy: $E_{Pt-H,app} = E_{Pt-H} - E_{Pt-H2O}$) by taking specific adsorption of interfacial water into consideration,

$$Pt{-}H_{ad} + H_2O \leftrightarrow Pt{-}H_2O{\downarrow}_{ad} + H^+ + e^- \quad (2)$$

and it is the $E_{Pt-H,\ app}$ that dictates the HER/HOR activity of Pt in aqueous solution.[33] Later, Goddard's group[34] drew the same conclusion based on DFT calculations. The compressive effect weakens the E_{Pt-H2O} if the H_2O binds the Pt electrode through the O (denoted as $H_2O{\downarrow}_{ad}$). If the E_{Pt-H2O} weakening dominates the E_{Pt-H} weakening upon compressive strain, the $E_{Pt-H,\ app}$ strengthens. As a result, the E_{peak} shifts positively toward high potential and the HER/HOR activity of Pt decreases, in agreement with our experimental observations (Figure 5C,D). In addition, the compressive strain induced positive shift of the H_{upd} peaks rules out the possibility that the decreased HER/HOR activity of the D-PtCu$_3$/C is caused by the compressive strain induced overweakening of the E_{Pt-H} *as per* the HBE theory; otherwise, the H_{upd} peak of the Pt(110) facet of D-PtCu$_3$/C would be located at a more negative potential than that of Pt(110) in acid (∼0.1 V).[15]

In accordance with the refined HBE theory, we recently proposed that the sharp H_{upd} peaks of Pt arise from the exchange between the H_{ad} and the specifically adsorbed water molecule with the oxygen facing toward the electrode (denoted as $H_2O{\downarrow}_{ad}$) (eq 2).[23] We further proposed that the sluggish HER/HOR activity of the Pt in base is caused by the too weak $E_{Pt-H2O{\downarrow}}$ for the interfacial water to effectively transport H_{ad} and OH_{ad} throughout the interface.[2] Our interpretation of the sharp H_{upd} peaks of Pt follows Koper et al.'s previous interpretation that the sharp H_{upd} peaks of stepped Pt surfaces arise from the exchange between the H_{ad} and the OH_{ad}[35] but differ in the oxygen species involved. In parallel, Koper's group recently stated that the sluggish HER/HOR activity of the Pt in base is caused by the too weak E_{Pt-OH}.[8] According to this statement, weakening E_{Pt-OH} by compressive strain will positively shift the E_{peak} toward high potential[36] and decrease the HER/HOR activity of Pt in a base, also in agreement with our experimental observations (Figure 5C,D). Despite the discrepancy of the oxygen species ($H_2O{\downarrow}_{ad}$ vs OH_{ad}) in exchange of H_{ad} as the cause of the sharp H_{upd} peaks of Pt(110), these arguments agree that the positive shift of the H_{upd} peaks of Pt(110) is caused by weakening the E_{Pt-O} rather than strengthening the E_{Pt-H} as shown here. The close relationship between the HER/HOR activity of stepped Pt surfaces in aqueous solution and the E_{peak} observed by Yan's group[15] is thus linked by the E_{Pt-O} rather than the E_{Pt-H}.

Therefore, the experimental results presented here that demonstrate the compressive strain decreasing rather than increasing the HER/HOR intrinsic activity of Pt in alkaline solution conclusively show that the HER/HOR activity of Pt is not solely governed by the E_{Pt-H}. In fact, they rather suggest that the sluggish HER/HOR kinetics of Pt in base is mainly limited by the overly weak E_{Pt-O}, in line with the latest arguments by Yan's,[33] Koper's,[8] and our groups.[2] Accordingly,

https://doi.org/10.1021/acscatal.1c01723
ACS Catal. 2021, 11, 8165−8173

the surface Ni or Ru induced improvements of the HER/HOR activity of Pt in a base is ascribed to their high oxophilicity (e.g., strong E_{Ni-O} and E_{Ru-O}).[4,5,8] It is, however, still under debate whether it is the binding between the Pt surface with the interfacial water (E_{Pt-H2O})[2,33] or the hydroxide (E_{Pt-OH})[6,8,37] that dictates the HER/HOR kinetics of Pt in a base. Advanced *in situ* characterization and mechanistic studies are needed to answer this question by identifying the roles of the oxygen species ($H_2O\downarrow$ and OH^-) during the HER/HOR.

The major finding here, that the compressive strain reduces the HER/HOR intrinsic activity of Pt in alkaline solution by weakening the E_{Pt-O} that is already too weak, has important implications toward the design of improved HER/HOR Pt-based catalysts. It suggests that the HER/HOR activity of Pt in alkaline solution can be effectively improved by either strengthening the E_{Pt-O} or decorating Pt surfaces with transition metals with the binding energy with oxygen stronger than E_{Pt-O}. Strengthening the E_{Pt-O} can be achieved via tensile strain by constructing M@Pt in which the M has a bigger atomic size than Pt, which is under investigation in our lab. This route, however, will strengthen the E_{Pt-H} that may be detrimental to the HER/HOR kinetics of Pt. This issue may be alleviated by constructing M_1@PtM_2 to tune the E_{Pt-H} and E_{M-O}, separately.

4. CONCLUSIONS

In this work we demonstrated that the compressive strain (1) reduces the HER/HOR intrinsic activity of Pt and (2) pushes the sharp H_{upd} peaks of the Pt(110) facet positively toward higher potentials in alkaline solution by constructing a relatively well-defined D-$PtCu_3$/C model with a core−shell Cu@Pt structure. These results led us to conclude that the HER/HOR of Pt in a base is limited by the overly weak Pt−O binding energy (E_{Pt-O}). The compressive strain is detrimental to the HER/HOR kinetics of Pt in a base by further weakening the E_{Pt-O}. Therefore, means to improve the HER/HOR intrinsic activity of Pt in a base include strengthening the E_{Pt-O} via tensile strain or ligand effects or depositing transition metals with high oxophilicity such as Ru and Ni.

5. EXPERIMENTAL METHODS

Chemicals. Carbon-supported platinum nanoparticles (Pt/C, 47.2 wt %) were purchased from Tanaka Kikinzoku Kogyo (TKK). Carbon-supported PtCu alloy nanoparticles ($PtCu_3$/C, 22.7 wt % Pt) were obtained from Johnson Matthey. Potassium hydroxide (KOH, 99.99%) and perchloride acid ($HClO_4$, 70%, PPT grade) were purchased from Sigma-Aldrich. All aqueous solutions were prepared using deionized (DI) water (18.2 MΩ·cm) obtained from an ultrapure purification system (Aqua Solution).

Working Electrode Preparation. The $PtCu_3$/C alloy (0.1 g) was added to 0.1 M $HClO_4$ solution (100 mL), stirred for 10 h at room temperature, and then collected by centrifuge and washed by DI water several times, until the solution had a pH of 7. The resultant nanoparticles were dried in a 40 °C vacuum overnight. The catalyst ink was prepared by mixing 2.0 mg of the above resultant catalyst powder, 1 mL of DI water, 1 mL of IPA, and 5 μL of 5 wt % Nafion solution. The mixture was sonicated for 45 min in an ice bath placed in the ultrasonicator. The well-dispersed ink was pipetted onto the cleaned and polished glassy carbon electrode and rotationally dried in air at room temperature with a 10 $\mu g/cm^2$ loading. For comparison, the Pt/C working electrode was prepared by the same procedures.

Electrochemical Measurements. All the electrochemical experiments were conducted using a three-compartment cell. The working electrode was 0.2463 cm^2 glassy carbon (Pine Instruments) with 10 $\mu g/cm^2$ thin-film catalyst. Pt mesh and Ag/AgCl (1 M Cl^-) were used as the counter and reference electrodes, respectively. All potentials reported in this work are referenced to the reversible hydrogen electrode (RHE), calibrated in the same electrode by measuring the potential of the HOR/HER currents at zero current corresponding to zero volts versus RHE (V_{RHE}).

The thin-film working electrodes were subjected to acid conditioning by potential cycling prior to electrochemical tests. The following actions were conducted in sequence: CV was obtained first in the fresh Ar-saturated 0.1 M $HClO_4$ solution, followed by ORR polarization curve measurements in O_2-saturated 0.1 M $HClO_4$ solution and then 0.1 M KOH. Lastly, HER/HOR polarization curves and then the CVs were collected on the same electrode in O_2/Ar-saturated 0.1 M KOH. Except for acid conditioning, all reactions were conducted with a 10 mV/s scan rate at room temperature. The details are as follows. (1) Acid conditioning: the thin-film electrodes were cleaned via potential cycling between 0.05 to 1.2 V_{RHE} with a scan rate of 500 mV/s for 100 cycles in an Ar-saturated 0.1 M $HClO_4$ solution. (2) After rinsing the working electrode in DI water, the CV was collected in Ar-saturated fresh 0.1 M $HClO_4$. (3) The ORR tests were conducted in O_2-saturated 0.1 M $HClO_4$ and 0.1 M KOH at a 1600 rpm rotation rate. The ORR performance based on the anodic scan was corrected by subtracting the CV collected in the Ar-saturated electrolyte. (4) The HER/HOR tests were conducted in a H_2-saturated 0.1 M KOH electrolyte with a potential range of −1.2 to 0 V vs Ag/AgCl and a rotation rate of 2500 rpm at room temperature. The CV was recorded in Ar-saturated 0.1 M KOH at the same potential range with a scan rate of 10 mV/s at a steady state. The HOR kinetic current density from the polarization curve based on the cathodic scan was normalized by the hydrogen mass transport using the Koutecky−Levich equation. All of the electrochemical active surface area was determined by integrating the hydrogen adsorption charge on the CV curves from 0.05 to 0.45 V by assuming a value of 210 $\mu C \cdot cm^{-2}$ for the adsorption of one hydrogen monolayer.

Impedance Measurements. The impedance spectra were recorded with frequencies from 10^5 to 0.1 Hz with an amplitude of 10 mV. Equivalent circuits were fitted to the data with Zview software. The solution resistances were measured at room temperature.

Microscopic Experiments. After acid conditioning, the thin-film D-$PtCu_3$/C catalysts on the working electrode were collected and dried in a 40 °C vacuum oven overnight and then sealed in vacuum vials before conducting microscopic experiments. The as-synthesized $PtCu_3$/C were observed without any pretreatment. EDS elemental maps were recorded at STEM mode with Thermo-Fisher Talos F200X at an accelerating voltage of 200 kV. Pt L and Cu K elemental maps were extracted, and overlaying maps was generated. High-angle annular dark-field (HAADF) STEM images were collected using a Hitachi HD2700C with the Cs probe corrector operated at 200 kV. The as-synthesized $PtCu_3$/C were observed without any pretreatment.

https://doi.org/10.1021/acscatal.1c01723
ACS Catal. 2021, 11, 8165−8173

XAS Experiments. The preparation of the catalyst electrode for *in situ* XAS experiments followed our previous study.[22,24] The Pt geometric loadings were made to give 0.5 transmission spectra edge heights at the Pt L_3 edge. A homemade flow half-cell circulated H_2-saturated 0.1 M KOH with three electrodes was used to provide the electrochemical environment. Prior to assembling the half-cell, the catalyst electrodes were immersed in 0.1 M $HClO_4$ under a weak vacuum for 1 h to clean the surface. The catalyst electrode was subjected to potential cycling between 0.05 to 1.1 V_{RHE} and then held to the proposed potential of 5 min to reach the steady-state before collecting XAS data in a fluorescence mode at 7-BM and 8-ID at the National Synchrotron Light Source II (NSLS II) (Brookhaven National Laboratory, NY, U.S.A.). All the experimental data were collected in conjunction with the appropriate reference foils for energy alignment and normalization. Typical experimental procedures were conducted with the details provided in our previous work.[24]

■ ASSOCIATED CONTENT

Supporting Information

The Supporting Information is available free of charge at https://pubs.acs.org/doi/10.1021/acscatal.1c01723.

HAADF-STEM images and intensity profiles (PDF)

■ AUTHOR INFORMATION

Corresponding Author

Qingying Jia − *Department of Chemistry and Chemical Biology, Northeastern University, Boston, Massachusetts 02115, United States;* orcid.org/0000-0002-4005-8894; Email: qjia@iit.edu

Authors

Li Jiao − *Department of Chemical Engineering, Northeastern University, Boston, Massachusetts 02115, United States;* orcid.org/0000-0002-1063-9313

Ershuai Liu − *Department of Chemistry and Chemical Biology, Northeastern University, Boston, Massachusetts 02115, United States;* orcid.org/0000-0002-6491-5504

Sooyeon Hwang − *Center for Functional Nanomaterials, Brookhaven National Laboratory, Upton, New York 11973, United States;* orcid.org/0000-0001-5606-6728

Sanjeev Mukerjee − *Department of Chemistry and Chemical Biology, Northeastern University, Boston, Massachusetts 02115, United States;* orcid.org/0000-0002-2980-7655

Complete contact information is available at: https://pubs.acs.org/10.1021/acscatal.1c01723

Author Contributions

Q.J. conceived the project. Q.J. designed the *in situ* XAS experiments and electrochemical experiments. L.J. conducted the *in situ* XAS experiments and electrochemical experiments and analyzed the data. E.L. conducted some of the XAS experiments. S.H. conducted STEM. Q.J. and S.M. supervised and advised the electrochemical experiments and data analysis. Q.J. and L.J. wrote the manuscript.

Notes

The authors declare no competing financial interest.

■ ACKNOWLEDGMENTS

This work was supported by the Office of Naval Research (ONR) under Award Number N00014-18-1-2155. This research used beamlines 7-BM (QAS) and 8-ID (ISS) of the National Synchrotron Light Source II, a U.S. Department of Energy (DOE) Office of Science User Facility operated for the DOE Office of Science by Brookhaven National Laboratory under Contract No. DE-SC0012704. This research used resources of the Center for Functional Nanomaterials, which is a U.S. DOE Office of Science Facility, at Brookhaven National Laboratory under Contract No. DE-SC0012704.

■ REFERENCES

(1) Durst, J.; Siebel, A.; Simon, C.; Hasché, F.; Herranz, J.; Gasteiger, H. A. New Insights into the Electrochemical Hydrogen Oxidation and Evolution Reaction Mechanism. *Energy Environ. Sci.* **2014**, *7* (7), 2255−2260.

(2) Liu, E.; Jiao, L.; Li, J.; Stracensky, T.; Sun, Q.; Mukerjee, S.; Jia, Q. Interfacial Water Shuffling the Intermediates of Hydrogen Oxidation and Evolution Reactions in Aqueous Media. *Energy Environ. Sci.* **2020**, *13* (9), 3064−3074.

(3) Liu, E.; Li, J.; Jiao, L.; Doan, H. T. T.; Liu, Z.; Zhao, Z.; Huang, Y.; Abraham, K. M.; Mukerjee, S.; Jia, Q. Unifying the Hydrogen Evolution and Oxidation Reactions Kinetics in Base by Identifying the Catalytic Roles of Hydroxyl-Water-Cation Adducts. *J. Am. Chem. Soc.* **2019**, *141* (7), 3232−3239.

(4) Li, J.; Ghoshal, S.; Bates, M. K.; Miller, T. E.; Davies, V.; Stavitski, E.; Attenkofer, K.; Mukerjee, S.; Ma, Z.-F.; Jia, Q. Experimental Proof of the Bifunctional Mechanism for the Hydrogen Oxidation in Alkaline Media. *Angew. Chem., Int. Ed.* **2017**, *56* (49), 15594−15598.

(5) Intikhab, S.; Rebollar, L.; Fu, X.; Yue, Q.; Li, Y.; Kang, Y.; Tang, M. H.; Snyder, J. D. Exploiting Dynamic Water Structure and Structural Sensitivity for Nanoscale Electrocatalyst Design. *Nano Energy* **2019**, *64*, 103963.

(6) Subbaraman, R.; Tripkovic, D.; Chang, K.-C.; Strmcnik, D.; Paulikas, A. P.; Hirunsit, P.; Chan, M.; Greeley, J.; Stamenkovic, V.; Markovic, N. M. Trends in Activity for the Water Electrolyser Reactions on 3d M (Ni, Co, Fe, Mn) Hydr (oxy) oxide Catalysts. *Nat. Mater.* **2012**, *11* (6), 550−557.

(7) Rebollar, L.; Intikhab, S.; Snyder, J. D.; Tang, M. H. Determining the Viability of Hydroxide-Mediated Bifunctional HER/HOR Mechanisms through Single-Crystal Voltammetry and Microkinetic Modeling. *J. Electrochem. Soc.* **2018**, *165* (15), J3209−J3221.

(8) McCrum, I. T.; Koper, M. T. M. The Role of Adsorbed Hydroxide in Hydrogen Evolution Reaction Kinetics on Modified Platinum. *Nat. Energy* **2020**, *5* (11), 891−899.

(9) Ledezma-Yanez, I.; Wallace, W. D. Z.; Sebastián-Pascual, P.; Climent, V.; Feliu, J. M.; Koper, M. T. M. Interfacial Water Reorganization as a pH-Dependent Descriptor of the Hydrogen Evolution Rate on Platinum Electrodes. *Nat. Energy* **2017**, *2*, 17031.

(10) Rebollar, L.; Intikhab, S.; Oliveira, N. J.; Yan, Y.; Xu, B.; McCrum, I. T.; Snyder, J. D.; Tang, M. H. Beyond Adsorption" Descriptors in Hydrogen Electrocatalysis. *ACS Catal.* **2020**, *10* (24), 14747−14762.

(11) Schwämmlein, J. N.; Stühmeier, B. M.; Wagenbauer, K.; Dietz, H.; Tileli, V.; Gasteiger, H. A.; El-Sayed, H. A. Origin of Superior HOR/HER Activity of Bimetallic Pt-Ru Catalysts in Alkaline Media Identified via Ru@Pt Core-Shell Nanoparticles. *J. Electrochem. Soc.* **2018**, *165* (5), H229−H239.

(12) Elbert, K.; Hu, J.; Ma, Z.; Zhang, Y.; Chen, G.; An, W.; Liu, P.; Isaacs, H. S.; Adzic, R. R.; Wang, J. X. Elucidating Hydrogen Oxidation/Evolution Kinetics in Base and Acid by Enhanced Activities at the Optimized Pt Shell Thickness on the Ru Core. *ACS Catal.* **2015**, *5* (11), 6764−6772.

(13) Wang, X.; Zhu, Y.; Vasileff, A.; Jiao, Y.; Chen, S.; Song, L.; Zheng, B.; Zheng, Y.; Qiao, S.-Z. Strain Effect in Bimetallic Electrocatalysts in the Hydrogen Evolution Reaction. *ACS Energy Lett.* **2018**, *3* (5), 1198−1204.

(14) Lu, S.; Zhuang, Z. Investigating the Influences of the Adsorbed Species on Catalytic Activity for Hydrogen Oxidation Reaction in Alkaline Electrolyte. *J. Am. Chem. Soc.* **2017**, *139* (14), 5156−5163.
(15) Sheng, W.; Zhuang, Z.; Gao, M.; Zheng, J.; Chen, J. G.; Yan, Y. Correlating Hydrogen Oxidation and Evolution Activity on Platinum at Different pH with Measured Hydrogen Binding Energy. *Nat. Commun.* **2015**, *6*, 5848.
(16) Zheng, J.; Sheng, W.; Zhuang, Z.; Xu, B.; Yan, Y. Universal Dependence of Hydrogen Oxidation and Evolution Reaction Activity of Platinum-Group Metals on pH and Hydrogen Binding Energy. *Sci. Adv.* **2016**, *2* (3), No. e1501602.
(17) Sheng, W.; Myint, M.; Chen, J. G.; Yan, Y. Correlating the Hydrogen Evolution Reaction Activity in Alkaline Electrolytes with the Hydrogen Binding Energy on Monometallic Surfaces. *Energy Environ. Sci.* **2013**, *6* (5), 1509−1512.
(18) Han, B.; Van der Ven, A.; Ceder, G.; Hwang, B.-J. Surface Segregation and Ordering of Alloy Surfaces in the Presence of Adsorbates. *Phys. Rev. B: Condens. Matter Mater. Phys.* **2005**, *72* (20), 205409.
(19) Li, M.; Zhao, Z.; Cheng, T.; Fortunelli, A.; Chen, C.-Y.; Yu, R.; Zhang, Q.; Gu, L.; Merinov, B. V.; Lin, Z.; et al. Ultrafine Jagged Platinum Nanowires Enable Ultrahigh Mass Activity for the Oxygen Reduction Reaction. *Science* **2016**, *354* (6318), 1414−1419.
(20) Schmidt, T. J.; Ross, P. N.; Markovic, N. M. Temperature Dependent Surface Electrochemistry on Pt Single Crystals in Alkaline Electrolytes: Part 2. The Hydrogen Evolution/Oxidation Reaction. *J. Electroanal. Chem.* **2002**, *524*−*525*, 252−260.
(21) Dutta, I.; Carpenter, M. K.; Balogh, M. P.; Ziegelbauer, J. M.; Moylan, T. E.; Atwan, M. H.; Irish, N. P. Electrochemical and Structural Study of a Chemically Dealloyed PtCu Oxygen Reduction Catalyst. *J. Phys. Chem. C* **2010**, *114* (39), 16309−16320.
(22) Jia, Q.; Li, J.; Caldwell, K.; Ramaker, D. E.; Ziegelbauer, J. M.; Kukreja, R. S.; Kongkanand, A.; Mukerjee, S. Circumventing Metal Dissolution Induced Degradation of Pt-Alloy Catalysts in Proton Exchange Membrane Fuel Cells: Revealing the Asymmetric Volcano Nature of Redox Catalysis. *ACS Catal.* **2016**, *6* (2), 928−938.
(23) Jiao, L.; Liu, E.; Mukerjee, S.; Jia, Q. In Situ Identification of Non-Specific Adsorption of Alkali Metal Cations on Pt Surfaces and Their Catalytic Roles in Alkaline Solutions. *ACS Catal.* **2020**, *10* (19), 11099−11109.
(24) Jia, Q.; Liang, W.; Bates, M. K.; Mani, P.; Lee, W.; Mukerjee, S. Activity Descriptor Identification for Oxygen Reduction on Platinum-Based Bimetallic Nanoparticles: In Situ Observation of the Linear Composition-Strain-Activity Relationship. *ACS Nano* **2015**, *9* (1), 387−400.
(25) Koh, S.; Strasser, P. Electrocatalysis on Bimetallic Surfaces: Modifying Catalytic Reactivity for Oxygen Reduction by Voltammetric Surface Dealloying. *J. Am. Chem. Soc.* **2007**, *129* (42), 12624−12625.
(26) Strasser, P.; Koh, S.; Anniyev, T.; Greeley, J.; More, K.; Yu, C.; Liu, Z.; Kaya, S.; Nordlund, D.; Ogasawara, H.; Toney, M. F.; Nilsson, A. Lattice-Strain Control of the Activity in Dealloyed Core-Shell Fuel Cell Catalysts. *Nat. Chem.* **2010**, *2*, 454.
(27) Kitchin, J. R.; Nørskov, J. K.; Barteau, M. A.; Chen, J. G. Role of Strain and Ligand Effects in the Modification of the Electronic and Chemical Properties of Bimetallic Surfaces. *Phys. Rev. Lett.* **2004**, *93* (15), 156801.
(28) Hammer, B.; Nørskov, J. K. In *Advances in Catalysis*; Academic Press: 2000; Vol. *45*, pp 71−129.
(29) Kitchin, J. R.; Nørskov, J. K.; Barteau, M. A.; Chen, J. G. Modification of the Surface Electronic and Chemical Properties of Pt(111) by Subsurface 3d Transition Metals. *J. Chem. Phys.* **2004**, *120* (21), 10240−10246.
(30) Alinezhad, A.; Gloag, L.; Benedetti, T. M.; Cheong, S.; Webster, R. F.; Roelsgaard, M.; Iversen, B. B.; Schuhmann, W.; Gooding, J. J.; Tilley, R. D. Direct Growth of Highly Strained Pt Islands on Branched Ni Nanoparticles for Improved Hydrogen Evolution Reaction Activity. *J. Am. Chem. Soc.* **2019**, *141* (41), 16202−16207.
(31) Sheng, W.; Gasteiger, H. A.; Shao-Horn, Y. Hydrogen Oxidation and Evolution Reaction Kinetics on Platinum: Acid vs Alkaline Electrolytes. *J. Electrochem. Soc.* **2010**, *157* (11), B1529−B1536.
(32) Tian, X.; Zhao, P.; Sheng, W. Hydrogen Evolution and Oxidation: Mechanistic Studies and Material Advances. *Adv. Mater.* **2019**, *31* (31), 1808066.
(33) Zheng, J.; Nash, J.; Xu, B.; Yan, Y. Perspective Towards Establishing Apparent Hydrogen Binding Energy as the Descriptor for Hydrogen Oxidation/Evolution Reactions. *J. Electrochem. Soc.* **2018**, *165* (2), H27−H29.
(34) Cheng, T.; Wang, L.; Merinov, B. V.; Goddard, W. A. Explanation of Dramatic pH-Dependence of Hydrogen Binding on Noble Metal Electrode: Greatly Weakened Water Adsorption at High pH. *J. Am. Chem. Soc.* **2018**, *140* (25), 7787−7790.
(35) Van der Niet, M. J.; Garcia-Araez, N.; Hernández, J.; Feliu, J. M.; Koper, M. T. Water Dissociation on Well-Defined Platinum Surfaces: the Electrochemical Perspective. *Catal. Today* **2013**, *202*, 105−113.
(36) Chen, X.; McCrum, I. T.; Schwarz, K. A.; Janik, M. J.; Koper, M. T. M. Co-Adsorption of Cations as the Cause of the Apparent pH Dependence of Hydrogen Adsorption on a Stepped Platinum Single-Crystal Electrode. *Angew. Chem., Int. Ed.* **2017**, *56* (47), 15025−15029.
(37) Strmcnik, D.; Uchimura, M.; Wang, C.; Subbaraman, R.; Danilovic, N.; Van Der Vliet, D.; Paulikas, A. P.; Stamenkovic, V. R.; Markovic, N. M. Improving the Hydrogen Oxidation Reaction Rate by Promotion of Hydroxyl Adsorption. *Nat. Chem.* **2013**, *5* (4), 300−306.

https://doi.org/10.1021/acscatal.1c01723
ACS Catal. 2021, 11, 8165−8173